JOURNAL OF SOLID STATE CHEMISTRY 83, 245–254 (1989)

A Niobium Phosphate Bronze Closely Related to the ITB Tungsten Bronzes: $K_7Nb_{14+x}P_{9-x}O_{60}$ ($x = 0.13$)

A. LECLAIRE,* A. BENABBAS, M. M. BOREL, A. GRANDIN, AND B. RAVEAU

Laboratoire de Cristallographie et Sciences des Matériaux, ISMRa, Campus 2, Boulevard du Maréchal Juin, 14032 Caen Cedex, France

Received March 13, 1989; in revised form June 12, 1989

A new niobium phosphate bronze $K_7Nb_{14+x}P_{9-x}O_{60}$ has been isolated and its structure has been determined by X-ray diffraction from a single crystal. It crystallizes in the orthorhombic system, space group *Pmma*, with $a = 36.883(3)$ Å, $b = 10.603(1)$ Å and $c = 6.4526(5)$ Å. The mixed framework of this bronze is closely related to the intergrowth tungsten bronzes (ITB): it consists of $[Nb_3P_2O_{13}]_\infty$ layers deduced from the ITB $[Mo_5O_{15}]_\infty$ layers observed in $Sb_2Mo_{10}O_{31}$ by replacing two octahedra out of five by PO_4 tetrahedra. Four such layers are stacked along **a**, sharing the corners of their polyhedra, forming $[Nb_{12}P_8O_{52}]_\infty$ slabs connected through $[NbP_2O_8]_\infty$ chains related to the perovskite and to the hexagonal tunnels. This host lattice determinates five types of tunnels of the brownmillerite and of the hexagonal tungsten bronzes, where the K^+ ions are located. © 1989 Academic Press, Inc.

Introduction

The association of PO_4 tetrahedra with octahedral structures allows mixed frameworks of corner-sharing octahedra and tetrahedra with anisotropic properties to be synthesized. Such materials are especially interesting when the octahedral element exhibits a mixed valence, leading to a possible delocalization of the electrons, i.e., the formation of bronzes. In this respect the phosphate tungsten bronzes (*1, 2*) form a very large family of metallic or semimetallic conductors in which perovskite slabs or ribbons are connected through PO_4 tetrahedra. Such materials can only be realized owing to the great flexibility of the perovskite framework which accommodates the PO_4 tetrahedra in various ways. Niobium, owing to its ability to take on the octahedral coordination and its role as a transition element susceptible to present two oxidation states Nb(V)/Nb(IV), should be considered as a potential candidate to form such mixed frameworks with metallic or semimetallic conductivity. The first phosphate niobium bronze $KNb_3P_3O_{15}$ (*3*) was indeed recently isolated. Its structure is very closely related to that of the tetragonal bronze (TTB) described by Magneli (*4*): it consists of TTB ribbons connected through PO_4 tetrahedra. These initial results have encouraged a more complete exploration of the system K–Nb–P–O. We report here on a new phosphate bronze $K_7Nb_{14+x}P_{9-x}O_{60}$ whose structure is closely related to those of the intergrowth tungsten bronzes (ITB) described by Hussain and Kihlborg (*5, 6*).

* To whom correspondence should be addressed.

0022-4596/89 $3.00
Copyright © 1989 by Academic Press, Inc.
All rights of reproduction in any form reserved.

Synthesis

The compound $K_7Nb_{14+x}P_{9-x}O_{60}$ was synthesized in a quantitative way for $0 \leq x \leq 0.13$ in two steps. First, an adequate mixture of K_2CO_3, $H(NH_4)_2PO_4$, and Nb_2O_5 was heated to 673 K in air in order to eliminate CO_2, H_2O, and NH_3. In the second step, the resulting finely ground product was mixed with an appropriate amount of niobium and sealed in an evacuated silica ampoule. This sample was then heated to 1373 K for 48 hr and quenched to room temperature.

Single crystals of this phase were prepared by a similar experimental method but starting from a different nominal composition KNb_4PO_{12} and using a longer annealing time, i.e., about 1 month, at 1373 K. Under these conditions black needles could be isolated from the mixture, whose composition, deduced from the structural determination $K_7Nb_{14.13}P_{8.87}O_{60}$, was confirmed by microprobe analysis.

The X-ray powder diffractogram, recorded with a Philips goniometer for Cu$K\alpha$ radiation, was indexed in the orthorhombic system (Table I), according to the parameters obtained from the single-crystal data (Table II). No variation in the cell dimension with x was observed.

TABLE I

$K_7Nb_{14.13}P_{8.87}O_{60}$: X-RAY POWDER PATTERN

h k l	d_{obs}	d_{calc}	I_{obs}	h k l	d_{obs}	d_{calc}	I_{obs}
1 0 1	6.362	6.356	14	0 2 2	2.755	2.756	40
2 0 1	6.109	6.091	5	7 0 2		2.751	
3 0 1	5.724	5.713	3	0 4 0	2.646	2.651	9
0 1 1	5.512	5.512	7	8 0 2		2.643	
0 2 0	5.296	5.302	17	10 3 0	2.550	2.552	17
4 0 1		5.287		4 4 0		2.548	
8 0 0	4.608	4.610	23	6 2 2	2.514	2.515	3
6 0 1	4.448	4.451	4	4 1 1		2.369	
0 2 1	4.092	4.096	14	10 1 2	2.368	2.367	6
6 2 0	4.008	4.015	5	8 2 2		2.366	
2 2 1		3.999		6 4 1	2.276	2.277	3
3 2 1	3.887	3.886	1	11 3 1		2.276	
7 1 1	3.805	3.809	2	0 5 0		2.121	
10 0 0	3.687	3.688	73	3 0 3	2.120	2.119	18
0 3 0	3.528	3.534	100	8 3 2		2.117	
7 2 1	3.230	3.234	9	18 0 0		2.049	
0 0 2		3.226		0 4 2	2.048	2.048	20
1 3 1	3.087	3.089	37	1 4 2		2.045	
0 1 2		3.087		15 0 2	1.953	1.956	4
11 0 1	2.975	2.975	5	18 0 1		1.953	
4 1 2	2.931	2.927	4	8 5 1	1.844	1.846	24
5 3 1	2.860	2.858	4	20 0 0		1.844	
6 0 2		2.857		20 1 0	1.818	1.817	3

TABLE II

SUMMARY OF CRYSTAL DATA, INTENSITY MEASUREMENTS, AND STRUCTURE REFINEMENT PARAMETERS FOR $K_7Nb_{14+x}P_{9-x}O_{60}$ ($x = 0.13$)

1. Crystal data	
Space group	*Pmma*
Cell dimensions (Å)	$a = 36.883(3)$
	$b = 10.603(1)$
	$c = 6.4526(5)$
Volume	$V = 2523.4(6)$
Z	2
2. Intensity measurements	
λ (Mo$K\alpha$)	0.71073 Å
Scan mode	ω–2/3 θ
SCan width (°)	0.8 + 0.35 tan θ
Slit aperture (mm)	1. + tan θ
Max θ (°)	45°
Standard reflections	3 measured every 2000 sec (no decay)
Reflections with $I > 3\sigma$	1257
μ (mm^{-1})	3.92
3. Structure solution and refinement	
Parameters refined	150
Agreement factors	$R = 0.035$, $R_w = 0.035$

Structure Determination

A dark plate crystal with dimensions $0.084 \times 0.072 \times 0.016$ mm was selected for the structure determination. The cell parameters reported in Table II were determined and refined by diffractometric techniques at 294 K with a least-squares refinement based upon 25 reflections with $18 < \theta < 22°$.

The data were collected on a CAD-4 Enraf–Nonius diffractometer with the data collection parameters reported in Table II. The reflections were corrected for Lorentz and polarization effect; no absorption corrections were performed.

Atomic coordinates of niobium atoms were deduced from the Patterson function and the other atoms were located by subsequent Fourier series. Refinement of the

atomic coordinates and the isotropic thermal factors of the oxygen atoms and the anisotropic thermal factors of the other atoms led to $R = 0.035$ and $R_w = 0.035$ and to the results in Table III.[1]

TABLE III

POSITIONAL PARAMETERS AND THEIR ESTIMATED STANDARD DEVIATIONS

Atom	x	y	z	B(Å^2)
Nb(1)	0.44489(3)	0.1762(1)	0.2429(2)	0.51(2)
Nb(2)	0.34236(3)	0.1775(1)	0.2539(3)	0.44(1)
Nb(3)	0.44584(7)	0.500	0.0173(3)	1.08(4)
Nb(4)	0.250	0.1830(2)	0.4548(3)	0.63(3)
Nb(5)	0.34155(6)	0.500	0.0438(3)	0.83(3)
P(1)	0.67583(9)	0.2380(3)	0.2473(8)	0.61(5)
P(2)	0.53909(8)	0.2367(3)	0.2548(8)	0.41(5)
P(3)	0.250	0.500	0.276(1)	0.4(1)
K(1)	0.6071(2)	0.000	0.256(1)	1.86(9)
K(2)	0.250	0.000	−0.042(1)	2.7(2)
K(3)	0.500	0.500	0.500	1.6(2)
K(4)	0.3885(2)	0.500	0.5326(9)	2.7(1)
K(5)	0.750	0.500	0.226(1)	2.8(2)
O(1)	0.3953(2)	0.1603(7)	0.235(2)	0.7(1)*
O(2)	0.4415(2)	0.3667(9)	0.205(1)	0.7(2)*
O(3)	0.5525(2)	0.1619(8)	0.069(1)	0.5(1)*
O(4)	0.4983(3)	0.2265(9)	0.272(2)	0.9(2)*
O(5)	0.5580(2)	0.1817(9)	0.446(1)	0.6(1)*
O(6)	0.4563(3)	0.000	0.255(3)	0.8(2)*
O(7)	0.3403(4)	0.000	0.291(2)	0.6(2)*
O(8)	0.6612(2)	0.1618(9)	0.060(1)	0.7(2)*
O(9)	0.6510(2)	0.2041(9)	0.434(2)	0.6(2)*
O(10)	0.3468(2)	0.3640(9)	0.224(2)	0.9(2)*
O(11)	0.2896(2)	0.1840(9)	0.275(1)	0.4(1)*
O(12)	0.5514(2)	0.3761(8)	0.237(2)	0.5(1)*
O(13)	0.500	0.500	0.000	1.6(5)*
O(14)	0.3905(4)	0.500	−0.036(2)	0.7(2)*
O(15)	0.2843(4)	0.500	0.124(2)	1.1(3)*
O(16)	0.6730(3)	0.377(1)	0.200(1)	1.1(2)*
O(17)	0.7148(2)	0.1996(9)	0.290(1)	0.6(2)*
O(18)	0.250	0.379(1)	0.425(3)	1.6(3)*
O(19)	0.250	0.000	0.486(4)	1.2(4)*

* These atoms were refined isotropically. Anisotropically refined atoms are given in the form of the isotropic equivalent displacement parameter defined as: $(\frac{4}{3}) \times [a2 \times B(1,1) + b2 \times B(2,2) + c2 \times B(3,3) + ab(\cos\gamma) \times B(1,2) + ac(\cos\beta) \times B(1,3) + bc(\cos\alpha) \times B(2,3)]$.

Description of the Structure and Discussion

The oxide $K_7Nb_{14}P_9O_{60}$ represents the fourth niobium phosphate characterized by a mixed valence of niobium. Two niobium phosphates $Nb_2P_3O_{12}$ (*7*) and $Na_{0.5}Nb_2P_3O_{12}$ (*8*) with a nasicon structure were indeed previously isolated besides the phosphate bronze $KNb_3P_3O_{15}$ (*3*). However, in this family only $KNb_3P_3O_{15}$ and $K_7Nb_{14}P_9O_{60}$ can be considered bronzes owing to the fact that their corner-sharing NbO_6 octahedra form ribbons which allow a delocalization of the electrons due to the mixed-valence Nb (IV)/Nb (V). On the other hand the nasicon phosphates are characterized by isolated NbO_6 octahedra and should not exhibit a metallic conductivity despite the existence of the mixed-valence Nb (IV)/Nb (V) in these compounds.

The host lattice of $K_7Nb_{14}P_9O_{60}$ is built up, like that of $KNb_3P_3O_{15}$, from corner-sharing PO_4 tetrahedra and NbO_6 octahedra in such a way that infinite chains of NbO_6 octahedra are connected through single PO_4 tetrahedra.

Three independent PO_4 tetrahedra must be distinguished. The P(1) and P(2) tetrahedra (Table IV) have a normal geometry characteristic of the monophosphate groups, i.e., characterized by P–O bonds close to 1.55 Å. On the opposite side the P(3) tetrahedron exhibits abnormally long P–O bonds equal to 1.60 Å; these distances are close to those observed in the NbO_4 tetrahedra belonging to a high-temperature form of Nb_2O_5 (*9*) and in the PO_4 tetrahedra of the oxide PNb_9O_{25} studied by Roth *et al.* (*10*); in this latter compound, the authors made the hypothesis that this phosphorus site was partly occupied by niobium. Our results observed here for the P(3) site are quite in agreement with the results obtained by these authors. We indeed observed that

[1] Lists of structure factors and anisotropic thermal motion parameters are available on request from the authors.

TABLE IV

DISTANCES (Å) AND ANGLES (°) IN THE PO_4 TETRAHEDRA

P(1)	O(8)	O(9)	O(16)	O(17)
O(8)	1.55(1)	2.48(1)	2.49(1)	2.50(1)
O(9)	106.2(5)	1.556(9)	2.51(1)	2.53(1)
O(16)	109.2(6)	109.9(5)	1.509(9)	2.50(1)
O(17)	109.3(5)	110.8(5)	111.3(5)	1.518(8)
P(2)	O(3)	O(4)	O(5)	O(12)
O(3)	1.521(9)	2.49(1)	2.45(1)	2.52(1)
O(4)	110.3(5)	1.513(8)	2.52(1)	2.53(1)
O(5)	106.8(4)	111.4(5)	1.535(9)	2.48(1)
O(12)	110.0(6)	111.4(4)	106.9(5)	1.550(8)
P(3)	O(15)	$O(15^{v})$	O(18)	$O(18^{iii})$
O(15)	1.60(1)	2.53(3)	2.65(2)	2.65(2)
$O(15^{v})$	104(1)	1.60(1)	2.65(2)	2.65(2)
O(18)	111.6(4)	111.6(4)	1.60(1)	2.56(3)
$O(18^{iii})$	111.6(4)	111.6(4)	106(1)	1.60(1)

during the refinement of the isotropic thermal factor of P(3), the *B* factor of this atom became negative. The multiplicity factor of this atom was then refined fixing the *B* factor at a positive value of 0.32 Å^2. After several iterative refinements a multiplicity of 1.24 was finally obtained with a normal *B* value for this atom. This multiplicity corresponds to the presence of about 18.5 electrons on the P(3) site, i.e., to occupancy factors of 0.864 and 0.136 for phosphorus and niobium, respectively. In order to check that such a phenomenon was not an artifact, another crystal was selected from another preparation, and new data were collected; the refinements led to identical results. Thus it can be summarized in a statistical manner that the P(3) sites are partly occupied by niobium.

The geometries of the five independent NbO_6 octahedra are almost the same (Table V). The NbO_6 octahedra are all distorted as shown from the O–O distances and O–Nb–O angles, which are spread over a wide range of values (Table V). Two sorts of octahedra can be distinguished, according to their neighboring polyhedra. Representatives of the first type of octahedron, Nb(2) and Nb(3), share their corners with four other NbO_6 octahedra and two PO_4 tetrahedra, whereas representatives of the second sort of octahedron, Nb(1), Nb(4), and Nb(5), share their corners with three other NbO_6 octahedra and three PO_4 tetrahedra. The Nb–O distances are in agreement with the valence bond theory developed by Brown and Wu (*11*). The Nb–O distances involving oxygen atoms common to two niobium atoms are generally shorter than those involving oxygen atoms common to one niobium atom and one phosphorus atom.

The view of the structure along **c** (Fig. 1) allows three sorts of infinite chains of polyhedra to be distinguished. Along **a**, infinite

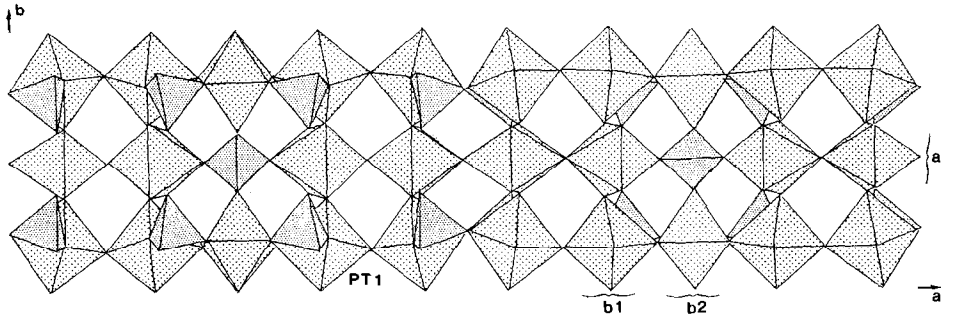

FIG. 1. Projection of $K_7Nb_{14}P_9O_{60}$ along **c** showing the infinite $[PNb_4O_{14}]_\infty$ chains (a), $[NbO_3]_\infty$ chains (b1), and $[Nb_2PO_8]_\infty$ chains (b2).

TABLE V

DISTANCES (Å) AND ANGLES (°) IN THE NbO_6 OCTAHEDRA

Nb(1)	O(1)	O(2)	O(3^{i})	O(4)	O(5^{ii})	O(6)
O(1)	1.838(8)	2.78(1)	2.75(1)	3.87(1)	2.69(1)	2.82(1)
O(2)	91.5(3)	2.039(9)	2.81(1)	2.61(1)	2.99(1)	3.94(1)
O(3^{i})	90.8(4)	87.5(4)	2.020(9)	2.97(1)	4.03(1)	2.73(2)
O(4)	169.4(3)	79.2(3)	93.8(4)	2.049(8)	2.80(1)	2.86(1)
O(5^{ii})	88.7(4)	95.1(4)	177.4(3)	87.2(3)	2.008(9)	2.77(1)
O(6)	97.5(4)	169.8(4)	87.6(6)	92.2(4)	89.9(6)	1.917(3)
Nb(2)	O(1)	O(7)	O(8^{i})	O(9^{ii})	O(10)	O(11)
O(1)	1.964(8)	2.67(1)	2.82(1)	2.77(1)	2.81(1)	3.92(1)
O(7)	87.5(4)	1.898(2)	2.84(1)	2.82(1)	3.89(1)	2.70(1)
O(8^{i})	89.7(3)	92.3(5)	2.038(9)	4.08(1)	2.84(1)	2.84(1)
O(9^{ii})	87.4(3)	91.1(5)	175.5(4)	2.046(9)	2.78(1)	2.89(1)
O(10)	90.3(3)	177.1(4)	89.4(4)	87.1(4)	1.994(8)	2.87(1)
O(11)	176.6(3)	89.2(5)	90.5(3)	92.5(3)	93.1(4)	1.952(6)
Nb(3)	O(2)	O(2^{iii})	O(12^{iv})	O(12^{i})	O(13)	O(14)
O(2)	1.867(9)	2.83(2)	3.95(1)	2.86(1)	2.90(1)	2.82(1)
O(2^{iii})	98.4(5)	1.867(9)	2.86(1)	3.95(1)	2.90(1)	2.82(1)
O(12^{iv})	169.1(4)	92.1(3)	2.103(9)	2.63(1)	2.77(1)	2.83(1)
O(12^{i})	92.1(3)	169.1(4)	77.3(5)	2.103(9)	2.77(1)	2.83(1)
O(13)	97.0(3)	97.0(3)	84.7(2)	84.7(2)	2.001(3)	4.04(1)
O(14)	91.3(4)	91.3(4)	85.3(4)	85.3(4)	167.2(4)	2.07(1)
Nb(4)	O(11)	O(11^{v})	O(17^{i})	O(17^{vi})	O(18)	O(19)
O(11)	1.863(7)	2.92(1)	2.82(1)	3.94(1)	2.71(1)	2.79(1)
O(11^{v})	103.2(5)	1.863(7)	3.94(1)	2.82(1)	2.71(1)	2.79(1)
O(17^{i})	90.1(3)	165.7(3)	2.106(8)	2.60(1)	2.95(1)	2.88(1)
O(17^{vi})	165.7(3)	90.1(3)	76.1(4)	2.106(8)	2.95(1)	2.88(1)
O(18)	86.4(4)	86.4(4)	89.4(4)	89.4(4)	2.09(1)	4.04(1)
O(19)	94.0(5)	94.0(5)	90.2(5)	90.2(5)	179.5(7)	1.951(4)
Nb(5)	O(10)	O(10^{iii})	O(14)	O(15)	O(16^{iv})	O(16^{i})
O(10)	1.862(9)	2.88(2)	2.74(1)	2.80(1)	3.95(1)	2.84(1)
O(10^{iii})	101.5(6)	1.862(9)	2.74(1)	2.80(1)	2.84(1)	3.95(1)
O(14)	94.1(4)	94.1(4)	1.88(1)	4.05(1)	2.88(1)	2.88(1)
O(15)	87.3(3)	87.3(3)	177.8(6)	2.18(1)	2.93(1)	2.93(1)
O(16^{iv})	165.7(4)	90.8(4)	92.3(4)	86.0(3)	2.115(9)	2.61(2)
O(16^{i})	90.8(1)	165.7(4)	92.3(4)	86.0(3)	76.1(5)	2.115(9)

Note. Symmetry code for Tables V and VI.

i: $1-x$;	y;	$-z$	viii: $\frac{1}{2}-x$; $-y$; z
ii: $1-x$;	y;	$1-z$	ix: $1-x$; $-y$; $-z$
iii:	x; $1-y$;	z	x: $x-\frac{1}{2}$; y; $-z$
iv: $1-x$;	$1-y$;	z	xi: x; y; $z-1$
v: $\frac{1}{2}-x$;	y;	z	xii: $1-x$; $1-y$; $1-z$
vi: $x-\frac{1}{2}$;	y;	$1-z$	xiii: x; y; $1+z$
vii:	x; $-y$;	z	xiv: $\frac{3}{2}-x$; $1-y$; z

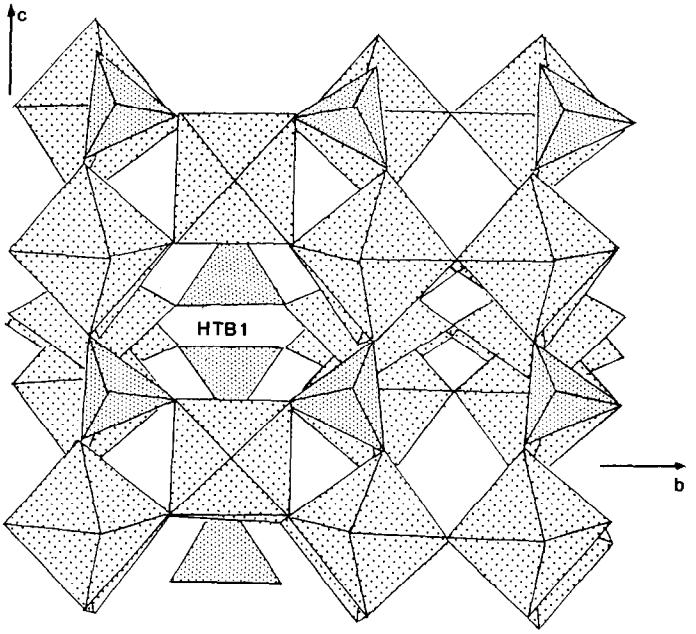

FIG. 2. Projection along **a** showing the $[NbPO_5]_\infty$ chains.

$[PNb_4O_{14}]_\infty$ chains are observed (labeled a) in which strings of four corner-sharing octahedra are connected through one PO_4 tetrahedron. Two types of chains $[NbO_3]_\infty$ and $[Nb_2PO_8]_\infty$ run along **b**. The first ones (labeled b1) consist of corner-sharing NbO_6 octahedra, whereas the second ones (labeled b2) are built up from groups of two corner-sharing NbO_6 octahedra linked through one single PO_4 tetrahedron. The projection of the structure onto the (100) plane (Fig. 2) shows that the host lattice $Nb_{14}P_9O_{60}$ also exhibits $[NbPO_5]_\infty$ chains running along **c**. Such chains, in which one PO_4 tetrahedron alternates with one MO_6, are often encountered in oxides characterized by a mixed framework of corner-sharing octahedra and tetrahedra, as shown for instance in $MoPO_5$ (*12*), $NaMoO_2PO_4$ (*13*), or $NaWO_2PO_4$ (*13, 14*). The most striking feature of this view of the structure along **a** is the geometry of the $[NbO_3]_\infty$ chains running along **b**. One indeed recognizes the 60–120° O–O–O angle characteristic of the hexagonal tungsten bronze structure (*4*) and the 90° O–O–O angle observed in the perovskite structure. In fact, the $Nb_{14}P_9O_{60}$ framework is formed by the stacking along **a** of $[Nb_3P_2O_{13}]_\infty$ layers which exhibit a close similarity to the ITB structures described by Hussain and Kihlborg (*5, 6*). These latter structures, which are observed for the formulation K_xWO_3 ($x < 0.10$) correspond to the intergrowth of the ReO_3-type structure with the hexagonal tungsten bronze framework (HTB). In the present case the $[Nb_3P_2O_{13}]_\infty$ layers are derived from the ITB host lattice $[Mo_5O_{15}]_\infty$ (Fig. 3) observed in $Sb_2Mo_{10}O_{31}$ (*15*) by replacing two octahedra out of five by PO_4 tetrahedra (Fig. 2). This results in two sorts of hexagonal rings in the $[Nb_3P_2O_{13}]_\infty$ layers: HTB rings similar to those observed in the hexagonal tungsten bronze structure and HBM rings similar to those observed in brownmillerite type oxides such as $Ca_2Fe_2O_5$ (Fig. 4) (*16*). The $[Nb_3P_2O_{13}]_\infty$ layers (Fig. 2) can thus be described as formed of single rib-

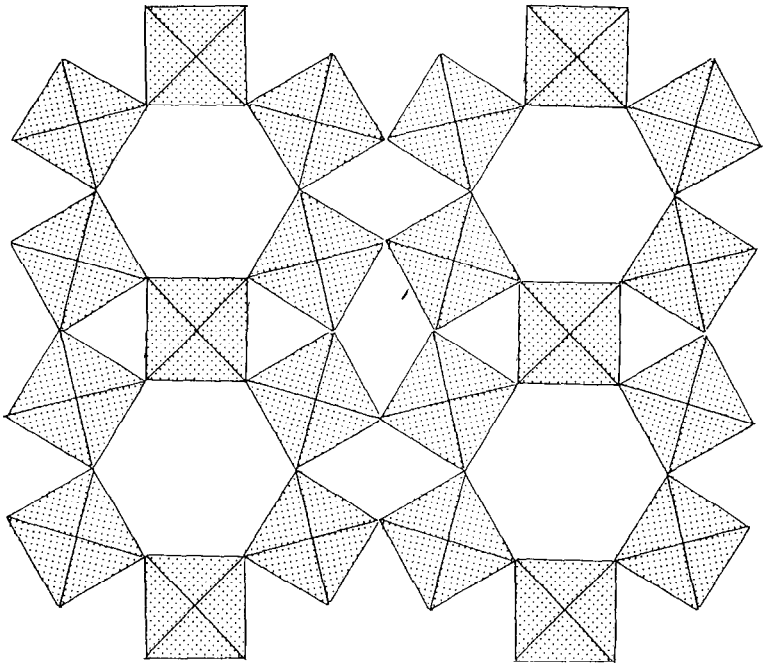

FIG. 3. An ITB structure: $Sb_2Mo_3O_{10}$.

bons of HTB rings running along **c** as in $Sb_2Mo_{10}O_{31}$ (Fig. 3b), connected through single ribbons of HBM rings running along **c**. Clearly, a bidimensional accord is observed along (100) between $K_7Nb_{14}P_9O_{60}$ and the member $Sb_2Mo_{10}O_{31}$ of the ITB series.

It is worth noting that the number of $[Nb_3P_2O_{13}]_\infty$ layers stacked between two successive $[Nb_2PO_8]_\infty$ chains must be even in order to ensure the connection between the different layers. Thus, the phosphate bronze $K_7Nb_{14}P_9O_{60}$ can be described by the formulation $[K_3Nb_6P_4O_{26}]_2 \cdot KNb_2PO_8$.

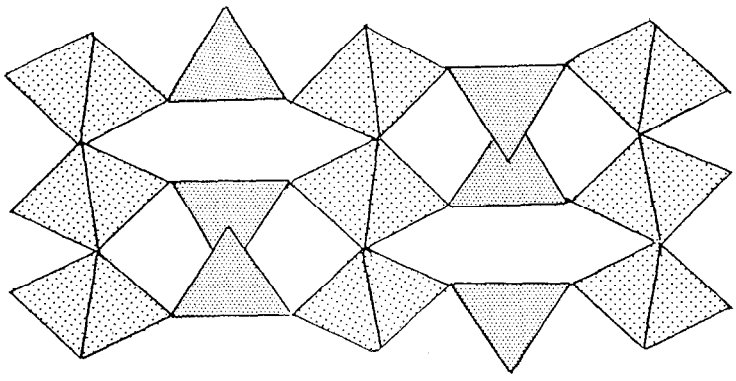

FIG. 4. The brownmillerite structure $Ca_2Fe_2O_5$ projected along **c** showing the HBM ring.

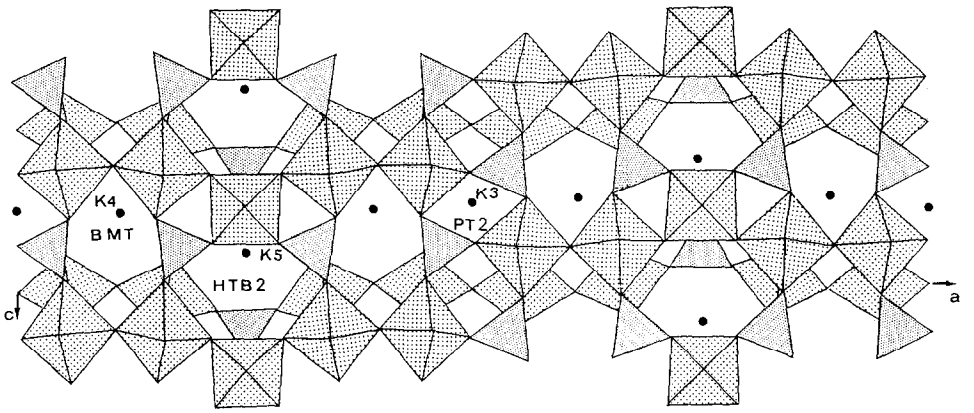

FIG. 5. Projection of $K_7Nb_{14}P_9O_{60}$ along **b** showing brownmillerite tunnels (BMT), HTB tunnels (HTB2) and perovskite tunnel (PT2).

This mixed framework delimits several types of tunnels which are similar to those observed in perovskite, HTB, and brownmillerite-type structures. Perovskite-type tunnels (labeled PT1 in Fig. 1) running along **c** intersect with brownmillerite tunnels (labeled BMT in Fig. 5) running along **b**. The potassium atoms K(1) are located at the intersection of these tunnels and exhibit an almost cubic eightfold coordination (Table VI, Fig. 6a). HTB-type tunnels are also observed running along **a** (labeled HTB1 in Fig. 2) and **b** (labeled HTB2 in Fig. 5). These tunnels are not absolutely straight,

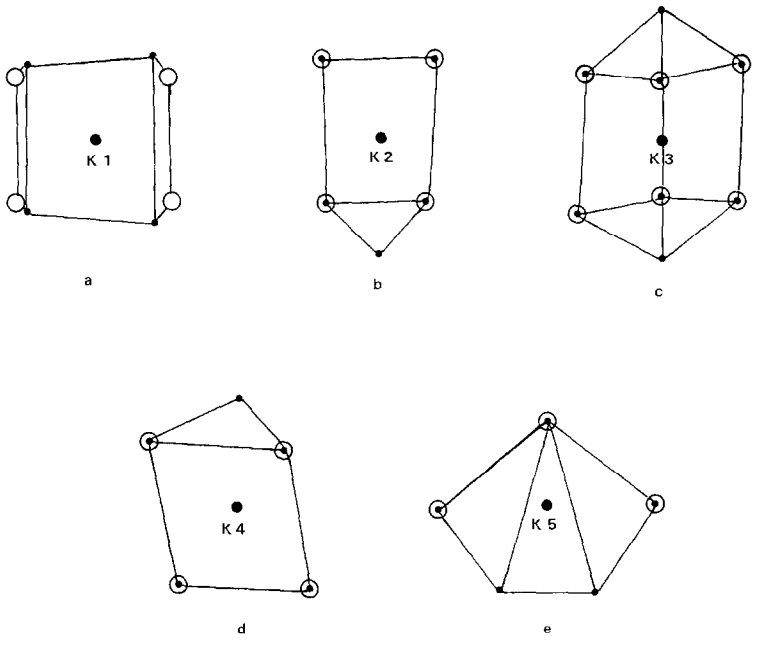

FIG. 6. The oxygen polyhedron around the potassium ion.

unlike those in HTB, but are waving along **a** and **b**, owing to the fact that the $[Nb_2PO_8]_\infty$ chains are slightly displaced along **c** at the junction between two $[Nb_{12}P_4O_{52}]_\infty$ slabs (Fig. 7). The K(5) atoms are located at the intersection of those tunnels, and exhibit an eightfold coordination (Fig. 6e) characterized by four close neighbors located at the corners of a tetrahedron and four farther neighbors forming a rectangle. In the same way the K(4) atoms are located at the intersection of the HTB1 and BMT tunnels: they are characterized by a ninefold coordination (Fig. 6d) forming a distorted monocapped square prism. Square tunnels derived from the perovskite type, built up of corner-sharing PO_4 tetrahedra and NbO_6 octahedra, (labeled PT2 in Fig. 5) run along **b**. Potassium atoms K(3) are located at the intersection of these PT2 tunnels and the HTB1 tunnels; they exhibit a 14-fold coordination with four close neighbors (Fig. 6c) delimiting a bicapped hexagonal prism. The K(2) atoms which lie in the HTB tunnels are surrounded by nine oxygen atoms (Fig. 6b).

Concluding Remarks

These results, as well as those obtained for the niobium phosphate bronze $KNb_3P_3O_{15}$, show definitively the great ability of niobium to form bronzes with a mixed framework, closely related to pure octahedral structures such as TTB, HTB, and ITB bronzes. It is worth pointing out that $K_7Nb_{14}P_9O_{60}$ should be considered the second member of a very large family which

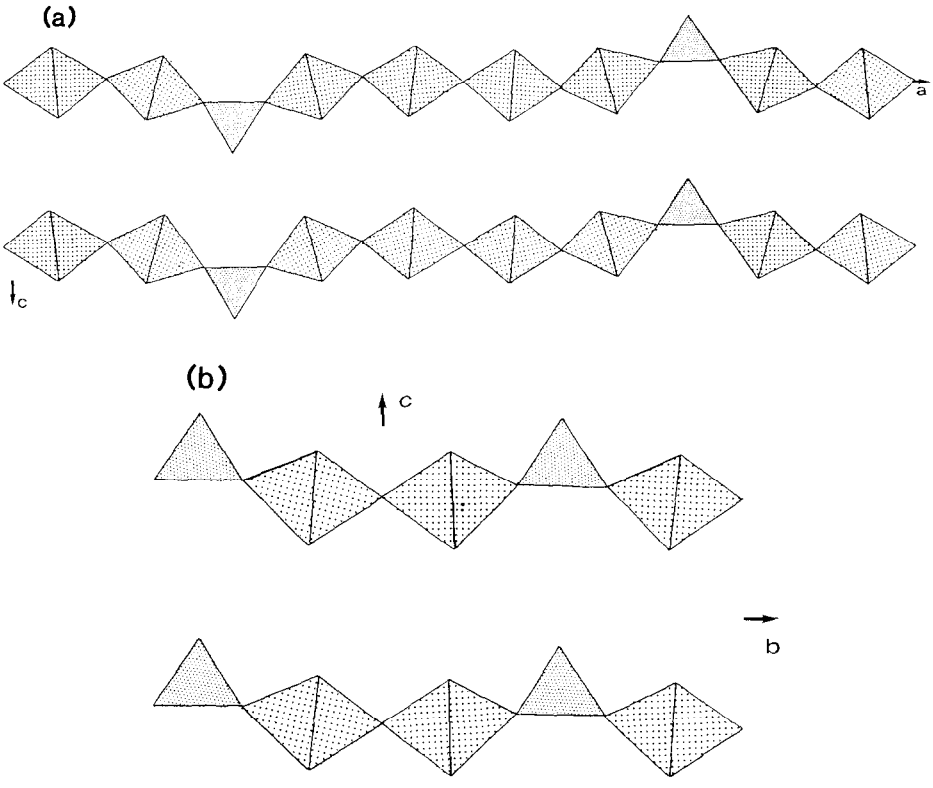

FIG. 7. The bottom and the top of an HBT1 tunnel (a), and an HTB2 tunnel (b), showing that they are not absolutely straight but are waving along the structure.

TABLE VI

THE K–O DISTANCES (Å) IN THE COORDINATION POLYHEDRA

K(1)–O(3)	= 2.909(10)	K(2)–O(11)	= 3.184(9)
K(1)–O(3^{vii})	= 2.909(10)	K(2)–O(11^{vii})	= 3.184(9)
K(1)–O(5)	= 2.915(9)	K(2)–O(11^{v})	= 3.184(9)
K(1)–O(5^{vii})	= 2.915(9)	K(2)–O(11^{viii})	= 3.184(9)
K(1)–O(8)	= 2.920(10)	K(2)–O(17^{ix})	= 2.952(9)
K(1)–O(8^{vii})	= 2.920(10)	K(2)–O(17^{i})	= 2.952(9)
K(1)–O(9)	= 2.937(9)	K(2)–O(17^{v})	= 2.952(9)
K(1)–O(9^{vii})	= 2.937(9)	K(2)–O(17^{x})	= 2.952(9)
		K(2)–O(19^{xi})	= 3.06(2)
K(3)–O(2)	= 3.207(8)	K(3)–O(4^{ii})	= 3.251(8)
K(3)–O(2^{xii})	= 3.207(8)	K(3)–O(4^{iii})	= 3.251(8)
K(3)–O(2^{ii})	= 3.207(8)	K(3)–O(12)	= 2.863(8)
K(3)–O(2^{iii})	= 3.207(8)	K(3)–O(12^{xii})	= 2.863(8)
K(3)–O(4)	= 3.251(8)	K(3)–O(12^{ii})	= 2.863(8)
K(3)–O(4^{xii})	= 3.251(8)	K(3)–O(12^{iii})	= 2.863(8)
		K(3)–O(13)	= 3.226(8)
		K(3)–O(13^{xiii})	= 3.226(8)
K(4)–O(2)	= 3.208(10)	K(5)–O(15^{iv})	= 2.587(14)
K(4)–O(2^{iii})	= 3.208(10)	K(5)–O(15^{i})	= 2.587(14)
K(4)–O(10)	= 2.900(10)	K(5)–O(16)	= 3.129(9)
K(4)–O(10^{iii})	= 2.900(10)	K(5)–O(16^{iii})	= 3.129(9)
K(4)–O(12^{xii})	= 2.978(9)	K(5)–O(16^{v})	= 3.129(9)
K(4)–O(12^{ii})	= 2.978(9)	K(5)–O(16^{xiv})	= 3.129(9)
K(4)–O(14^{xiii})	= 2.783(12)	K(5)–O(18^{xii})	= 2.594(15)
K(4)–O(16^{xii})	= 3.131(10)	K(5)–O(18^{ii})	= 2.594(15)
K(4)–O(16^{ii})	= 3.131(10)		

Note. See note to Table V for symmetry code.

can be formulated $(K_3Nb_6P_4O_{26})_n$ KNb_2PO_8. Moreover the possible intergrowths of this structural type with the ITB bronzes which exhibit a bidimensional structure should be considered. Thus, a new route is opened to the generation of microphases with a tunnel structure and a bronze character. The electron transport properties of these materials will be investigated.

References

1. B. RAVEAU, *Proc. Indian Natl. Sci. Acad. Part A* **52,** 67 (1986).
2. B. RAVEAU, *Proc. Indian Acad. Sci. Chem Sci.* **96,** 419 (1986).
3. A. LECLAIRE, M. M. BOREL, A. GRANDIN, AND B. RAVEAU, *J. Solid State Chem.* **80,** 12 (1989).
4. A. MAGNELI, *Ark. Kemi* **1,** 213 and 269 (1949).
5. A. HUSSAIN AND L. KIHLBORG, *Acta Crystallogr. A* **32,** 551 (1976).
6. A. HUSSAIN, *Chem. Scr.* **11,** 224 (1977).
7. A. LECLAIRE, M. M. BOREL, A. GRANDIN, AND B. RAVEAU, *Acta Crystallogr. C* **45,** 699 (1989).
8. A. LECLAIRE, M. M. BOREL, A. GRANDIN, AND B. RAVEAU, *Mater. Res. Bull.*, in press.
9. B. M. GATEHOUSE AND A. D. WADSLEY, *Acta Crystallogr.* **17,** 1545 (1964).
10. R. S. ROTH, A. D. WADSLEY, AND S. ANDERSSON, *Acta Crystallogr.* **18,** 643 (1965).
11. I. D. BROWN AND K. K. WU, *Acta Crystallogr. B* **32,** 1957 (1976).
12. P. KIERKEGAARD AND J. M. LONGO, *Acta Chem. Scand.* **24,** 427 (1970).
13. P. KIERKEGAARD, *Ark. Kemi* **18,** 553 (1962).
14. P. KIERKEGAARD, *Ark. Kemi* **19,** 51 (1962).
15. M. PARMENTIER, C. GLEITZER, A. COURTOIS, AND J. PROTAS, *Acta Crystallogr. B* **35,** 1963 (1979).
16. E. F. BERTAUT, P. BLUM, AND A. SAGNIERES, *Acta Crystallogr.* **12,** 149 (1959).